Building and Environment 237 (2023) 110327

Contents lists available at ScienceDirect

Building and Environment

journal homepage: www.elsevier.com/locate/buildenv

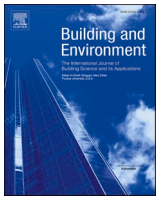

# Sensitivity analysis and weather condition effects on hygrothermal performance of green roof models characterized by recycled and artificial materials' properties

Mostafa Kazemi [a,*], Ramin Rahif [b], Luc Courard [a], Shady Attia [b]

[a] GeMMe Building Materials, Department of Urban and Environmental Engineering (UEE), Faculty of Applied Sciences, University of Liège, 4000, Liège, Belgium
[b] Sustainable Building Design (SBD) Lab, Department of Urban and Environmental Engineering (UEE), Faculty of Applied Sciences, University of Liège, 4000, Liège, Belgium

ARTICLE INFO

*Keywords:*
Weather condition
Local and global methods
Heat flux
Coarse granular aggregates
Green roof layers

ABSTRACT

This study conducted a sensitivity analysis and assessed the effects of long-term weather conditions on green roof models, including recycled and artificial materials. Climate conditions can affect the hygrothermal performance of green roof materials, but this important issue has hardly been evaluated for drainage and substrate layers made of recycled and artificial materials. Climate change makes it unclear how well green roofs will perform hygrothermally. Moreover, the heat flux sensitivity to the thickness and physical characteristics of green roofs with artificial and recycled materials has received less attention. This study applied three weather scenarios on green roof models with artificial and recycled materials: the beginning, middle, and end of the 21st century. As per the results, at the beginning and middle of the 21st century, substrate layers' water content was roughly nine times more than the drainage layers'. At the end of the 21st century, the comparable difference was 6.5 times larger. During the summer and the beginning of autumn, the green roofs' thermal performance with recycled and artificial materials was improved until the end of the 21st century. The entire parameter change demonstrated the scatter of thermal conductivity, density, and thickness effectively influenced the dispersion of heat flux for the green roof layers. Also, the scatter of density was more effective in heat flux dispersion for substrate layer than drainage layer.

## 1. Introduction

Green roofs' ability to provide thermal protection may help buildings to use less energy and experience less thermal load [1–4]. Also, the configuration (thickness) of drainage and substrate layers and their materials' thermal and physical properties can affect the insulation performance and water-holding capacity of green roof systems [5–7]. On the other hand, since green roofs with different materials' characteristics can be highly affected by climate conditions [8–12], their thermal performance and workability have been assessed under different weather conditions. Regarding this, Getter et al. [13] compared the performance of green roofs with traditional gravel roofs in a Mid-western U.S. climate with hot, humid summers and cold, snowy winters. The heat flux from the building was lower for the green roof than the gravel roof, even under chilly and wet conditions. The gravel roof consistently experienced more extreme maximum and minimum average monthly temperatures and heat fluxes than the green roof over a year. Green roofs' effects on heat fluxes and surface temperatures during the winter were assessed by Stella and Personne [14] in a temperate climate. The results showed green roofs decreased heat flux fluctuations at the building surface. Also, the building surface's temperature and heat flux variations were lessened by deeper substrates.

The thermal, hydrodynamic, and physical characteristics and thickness of green roof materials and layers play a fundamental role in hygrothermal performance of roofing systems [6,15]. Scharf and Zluwa [16] investigated different green roof systems' building physical

*Abbreviations:* SC, Substrate without coarse recycled materials (Control Substrate); SP, Substrate with coarse recycled materials (Proposed Substrate); RH, Relative Humidity; COV, Coefficient Of Variation; TMY, Typical Meteorological Year; RCA, Recycled Coarse Aggregate; LECA, Lightweight Expanded Clay Aggregate; NCA, Natural Coarse Aggregate; IMSWA, Incinerated Municipal Solid Waste Aggregate.

* Corresponding author.
*E-mail addresses:* mostafa.kazemi@uliege.be (M. Kazemi), ramin.rahif@uliege.be (R. Rahif), luc.courard@uliege.be (L. Courard), shady.attia@uliege.be (S. Attia).

https://doi.org/10.1016/j.buildenv.2023.110327
Received 5 February 2023; Received in revised form 13 April 2023; Accepted 17 April 2023
Available online 19 April 2023

properties. They concluded that the thicker the green roof construction was, the better the building's physical properties were. However, it was unreliable to estimate the average U-value of green roofs based only on construction thickness. When paired with a drainage layer with a high pore volume, substrate materials with a high-water storage capacity improved the building's physical characteristics. Zhang et al. [17] carried out a sensitivity analysis on green roof systems. The results showed that the rate at which the green roof reduced cooling load rose as insulation effectiveness declined owing to an increase in the inward heat flux. Mechelen et al. [18] revealed that small amounts of irrigation were needed for green roofs in temperate climate to have a more sustainable future for urban life. A study was done by Chan and Chow [19] on green roof performance under future climate conditions. According to the results, in comparison to the base case, the building case with soil thickness of 0.4 m and plant height of 0.05 m kept the energy consumption no more or less than the current level, ranging from −2.4% to −10%.

The recycled materials have been found to work well for commercial green roofs [20]. Regarding this, Eksi et al. [21] showed that the particle dispersion of zeolite prevented it from supporting plant growth, despite performing well in terms of nutrient and water retention. Concrete as the coarse and heavy material performed well as a substrate for the plant growth. Cascone [22] revealed that rubber crumbs had the greatest density and thermal conductivity measurements of all the drainage materials analyzed. Mickovski et al. [23] found that the green roof substrate made from recycled inert construction waste material was effective in providing good drainage, promoting plant development, and being resistant to slippage and erosion. Substrates made from a combination of recycled red brick and clay pellets were very promising for maximizing plant diversity of green roof systems as reported by Molineux et al. [24]. A study by Bates et al. [25] demonstrated for green roof plant diversity, the crushed brick or recycled aggregates with a high proportion of crushed brick were ideal for substrate materials. Also, recycled bricks and cork were introduced by Tams et al. [7] as promising green roof materials. Rincón et al. [26] revealed that, compared to pozzolana as a drainage material for green roof systems, recycled rubber showed a lower environmental impact. Shafique et al. [27] reported that recycled materials in green roof layers might decrease the environmental impacts. However, the use of by-products and recycled materials for green roof layers should be studied more deeply as recommended by Scolaro and Ghisi [28].

Long-term experimental and modeling efforts have been conducted by Kazemi et al. [5,6,9,29,30] to evaluate the hygrothermal, physical, and configuration of the drainage layer and substrate of green roofs made of artificial and recycled components. Kazemi et al. [5] suggested three commercial drainage materials as artificial and recycled production: Lightweight Expanded Clay Aggregate (LECA), Incinerated Municipal Solid Waste Aggregate (IMSWA), and Recycled Coarse Aggregate (RCA). Their results were compared with Natural Coarse Aggregate (NCA) as a control coarse granular aggregate. For the substrate layer, the results of a commercial substrate material, including coarse recycled materials (SP), were compared with those of the control substrate without coarse recycled materials (SC). Based on heat flow measurement results and hygrothermal modeling outputs, Kazemi and Courard [6] demonstrated that a 15-cm SP and a 15-cm SC in a wet state differed marginally from one another (4.3%). The respective difference in the dry state was slightly more (6.4%) [30]. Also, 5-cm RCA and 5-cm NCA both had the same Rc-value [6]. In a wet state, considering the substrate and drainage layers together, there was a slight variation between the RC values of the green roof with 15-cm SP and 5-cm RCA and the green roof with 15-cm SC and 5-cm NCA (4.2%) [6]. The corresponding difference in the dry state was 5.3%, as presented by Kazemi et al. [30]. Following that, measurements and presentations of three key indicators, including Rc-value, water permeability, and water retention capacity, were made by Kazemi et al. [5] for different substrate and drainage materials, and their outputs were compared with each other. The results showed that in comparison to SP, the water retention capacity of SC was nearly 1.2 times. The corresponding difference for water permeability test was 1.5 times. However, the values of water retention capacity and water permeability for both SC and SP were in the required ranges given by FLL guidelines [31]. For drainage materials, when compared to NCA, LECA and IMSWA's water retention capacity values were roughly two times higher. Also, the respective value for RCA was around 1.5 times higher. 5-cm LECA obtained the highest Rc-value among coarse granular drainage materials.

Based on the above, it is evident that certain research on the measurement of water retention capacity, water permeability, and heat flow, across green roof layers, including coarse artificial and recycled materials, has been conducted. Although the hygrothermal performance of green roof materials can be influenced by climate conditions [8,10,11], this critical issue has scarcely been assessed for drainage and substrate layers including artificial and recycled components. Thus, there is a lack of understanding of the hygrothermal performance of green roof layers including artificial and recycled materials in the future till end of 21st century when the weather conditions will change. On the other hand, green roof layers' thermal resistance is more sensitive to some parameters that must be taken into account [17]. This issue has received less attention for green roof layers, including artificial and recycled materials.

Therefore, in this study, different weather data scenarios for the 21st century were supposed and applied to the validated green roof models. The research aims to answer the following two questions:

1-What is the influence of using artificial and recycled materials on green roof performance under the temperate climate of Liege city till the end of the 21$^{st}$century?
2-To what extent is green roofs' thermal resistance sensitive to parameters of drainage and substrate layers, including artificial and recycled components?

To answer those questions, the hygrothermal performance of drainage and substrate layers, including different coarse artificial and recycled components, was assessed. Moreover, analytical methods were used to evaluate green roofs' thermal resistance sensitivity to the configuration (thickness) and physical characteristics of drainage and substrate layers made with artificial and recycled components.

This study supposed three weather data scenarios: beginning, middle, and end of the 21st century. Considering this, the novelty of this research lies in considering different climate scenarios for the 21st century to apply to green roof models characterized by recycled and artificial materials' properties. The effect of weather data scenarios on heat flux values and water content of green roof layers was assessed and compared to each other. Also, conducting a sensitivity analysis on green roof layers based on the properties of artificial and recycled materials is another novelty of this study.

## 2. Materials and methods

In this study, three weather data scenarios: beginning, middle, and end of the 21st century, were supposed and applied to the validated green roof models, including coarse artificial and recycled. Then, the heat flux and water content variations for different layers and materials were compared to each other through the end of the 21st century. After that, the sensitivity of heat flux value to green roof layers' thickness and materials properties was assessed using analytical methods.

### 2.1. Configuration and characteristics of green roof layers

This study mainly focused on green roof models with substrate and drainage layers, as coarse artificial and recycled aggregates could be used only for these two layers of green roof systems. As Kazemi et al. (Kazemi et al., 2023) suggested, three commercial drainage materials: RCA, IMSWA, and LECA were considered where NCA was supposed to

control coarse granular aggregate. IMSWA included the crushed brick, crushed glass, crushed aggregate, inert waste, and crushed ceramic. For the substrate layer, the results of SP were compared with SC. SP was composed of recycled tiles and bricks and organic matter, while no recycled materials were used for SC. As per Fig. 1, the substrate and drainage layers' thicknesses were intended to be 15 cm and 5 cm, respectively, as considered by Kazemi et al. [6,29,30]. Green roof materials' properties, introduced to the WUFI software for the validation of green roof models, are presented in Table 1. Note that, to separate substrate and drainage layers from each other, a thin filter layer was used in green roof specimens [6,30]. This thin filter layer was not modeled in the simulation as it was not needed to be considered for substrate and drainage layers separation and it didn't affect the hygrothermal performance of green roof models.

For validation, the depth-based temperature changes within green roof models with the IMSWA and LECA drainage layers were compared with experimental outputs measured by Kazemi et al. [5,29]. The outputs of green roof models with the drainage layer of RCA and NCA have already been validated by Kazemi and Courard [6] in which nearly the same as what was shown for the green roof specimens, the general trend of the temperature distribution through the green roof models' depth was seen.

### 2.2. Boundary conditions and weather data

According to the Regional Climate Model (MAR) "Modèle Atmosphérique Régional" [32], the Typical Meteorological Year (TMY) data file was used to apply weather condition of Liège to green roof models. Liège is a city in Belgium, located at 50°38′23″ N 05°34′14″ E. Considering that TMYs as data sets of hourly values are fairly accurate and practical in projecting long-term building energy and thermal performance [33], they are frequently employed by those who design and model buildings [34]. In this study, different weather parameters were incorporated in the TMYs data files, including solar radiation, air temperature, RH, rain, etc. The weather data were applied to the top of green roof models using WUFI software. For the interior surface, the initial conditions were considered based on EN 15026 [35] as provided by WUFI software. According to EN 15026 [35], the daily mean of the external air temperature was automatically entered into the graph in Fig. 2 to produce the inside air conditions. This simplified approach was suggested only for dwellings and offices to determine the internal temperature and RH for heated buildings. Also, since Liège city has a temperate climate, a high moisture load of RH was supposed for the interior surface.

As presented in Table 2, three weather scenarios were considered in this study to apply to green roof models. Scenario 1 was based on historical observations between 2001 and 2020. Scenarios 2 and 3 were the predicted weather data for the middle (2040–2060) and end (2080–2100) of the 21st century. In Appendix 1, an average of one year was taken from 20 years for each scenario to apply to green roof models. To present the trends of weather data curves in Appendix 1, solid lines with an average value of 200 points were generated. The solar radiation and air temperature had a similar trend, where their lowest amounts were observed from November (end of autumn) until March (beginning of spring) for all scenarios. The highest RH for scenario 1 was in March, while scenarios 2 and 3 experienced the highest RH in December. For all scenarios, the lowest amount of RH occurred between Jun and September, when solar radiation and air temperature were high. The highest rainfall averagely occurred at the end of autumn, during winter, and at the beginning of spring. Also, the lowest rainfall was observed during summer and at the beginning of autumn. The average value of RH for all scenarios was the same (76%). The average value of rainfall for scenarios 1 and 2 (0.022 Ltr/m$^2$) was more than that for scenario 3 (0.015 Ltr/m$^2$). The temperatures for scenarios 1, 2, and 3 averagely were 10.7, 11.6, and 12.2 °C, respectively. The average solar radiation values for the same scenarios were 23.7, 25.7, and 21 W/m$^2$.

### 2.3. Sensitivity analysis (local and global methods)

Since the hygrothermal behavior of green roof systems is highly dependent on the characteristics and thickness of substrate and drainage materials [6,15], analytical methods were used to evaluate green roofs' heat flux sensitivity. The approach of sensitivity analysis in this study was similar to the work done by Mahar et al. [36]. This study considered some parameters (independent variables), including thermal conductivity in a dry state ($\lambda_0$), water content (W), density ($\rho$), and thickness of substrate and drainage layers (L), and then, their effects were evaluated on the heat flux, q (dependent variable). Both local and global sensitivity analyses were taken into account in this study. In the local method, a single independent variable was changed, and others were assumed to be constant. The global method examined the sensitivity regarding the entire parameters change.

As presented in Table 3, the maximum and minimum of $\lambda_0$ value for drainage and substrate layers was determined based on a variation of green roof materials' thermal properties given by Kazemi et al. [5]. Considering that coarse granular aggregates were used for the drainage layer by Kazemi et al. [6,30], its minimum thickness shouldn't be supposed less than 4 cm to easily dewater green roof systems [8,37]. Also, its maximum thickness was assumed 6 cm to prevent applying more load to rooftops as recommended [30,38]. On the other hand, since the substrate depth of the green roof, at 15 cm, can offer an acceptable depth for a variety of plant growth [39], and in some cases, a 9-cm substrate can adequately provide plant growth depth, 15 cm, and 9 cm were supposed as the maximum and minimum thicknesses of the substrate layer, respectively. According to the water retention capacity of green roof materials given by Kazemi et al. [5], the maximum water content of drainage and substrate materials was determined. As per the weight of green roof materials [5], the maximum and minimum density of drainage and substrate components was chosen.

After determining the maximum, minimum, mean value, and standard deviation for materials' properties, it was required to generate the random values belonging to the distribution of each independent

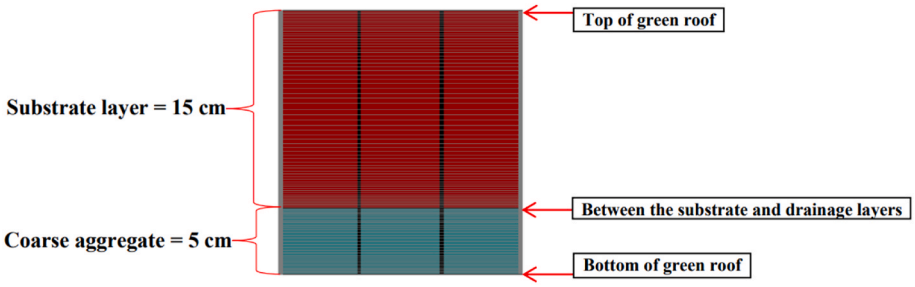


**Fig. 1.** Two-dimensional green roof model built using WUFI software. (For interpretation of the references to color in this figure legend, the reader is referred to the Web version of this article.)

**Table 1**
Green roof materials' properties.

| Green roof layers | Materials | Density (kg/m$^3$) | Porosity | Specific heat capacity, dry (J/kg K) | Thermal conductivity, dry (W/m·K) | Water vapour diffusion resistance factor | Reference water content (kg/m$^3$) | Free water content (kg/m$^3$) | Water absorption coefficient (kg/m$^2$.s$^{0.5}$) |
|---|---|---|---|---|---|---|---|---|---|
| Substrate layer | SC [6] | 1075 | 0.48 | 880 | 0.15 | 3.62 | 10.31 | 380.95 | 0.47 |
| | SP [6] | 1001 | 0.486 | 810 | 0.16 | 3.35 | 7.73 | 285.71 | 0.22 |
| Drainage layer | NCA [6] | 1437 | 0.42 | 770 | 0.114 | 1 | 1.16 | 42.86 | 0.03 |
| | RCA [6] | 1165 | 0.50 | 730 | 0.11 | 1 | 3.32 | 122.76 | 0.07 |
| | IMSWA [29] | 1147 | 0.47 | 750 | 0.115 | 1 | 2.74 | 101.2 | 0.07 |
| | LECA [5] | 439 | 0.55 | 710 | 0.067 | 1 | 2.83 | 141 | 0.11 |

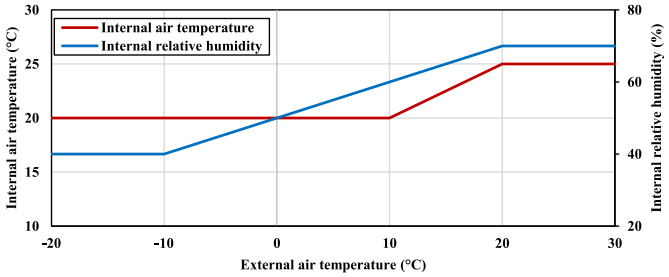


**Fig. 2.** Dwellings and office buildings' daily mean internal air temperature and RH depending on daily mean external air temperature.

**Table 2**
Weather data files' scenarios.

| No. | Scenarios | Type | Years |
|---|---|---|---|
| 1 | Beginning of the 21st century | Historical observation | 2001–2020 |
| 2 | Middle of the 21st century | Predicted | 2040–2060 |
| 3 | End of the 21st century | Predicted | 2080–2100 |

**Table 3**
Values of independent variables for drainage and substrate layers.

| Green roof layer | Independent variables | Max | Min | Mean (μ) | Standard deviation (σ) |
|---|---|---|---|---|---|
| Drainage layer | $\lambda_0$ | 0.15 | 0.05 | 0.1 | 0.0167 |
| | L | 0.06 | 0.04 | 0.05 | 0.0033 |
| | W | 200 | 0 | 100 | 33.333 |
| | ρ | 1500 | 400 | 950 | 183.333 |
| Substrate layer | $\lambda_0$ | 0.3 | 0.1 | 0.2 | 0.033 |
| | L | 0.15 | 0.09 | 0.12 | 0.01 |
| | W | 500 | 0 | 250 | 83.33 |
| | ρ | 1400 | 800 | 1100 | 100 |

variable. To increase the accuracy of distribution, 5000 random values were generated for each independent variable. To achieve this goal, the normal distribution function (f (x, μ, $\sigma$)) was used, as shown in Eq. (1). The value of this function was between 0 and 1.

$$f(x,\mu,\sigma)=\frac{1}{\sqrt{2\pi}\,.\,\sigma}e^{\frac{-(x-\mu)^2}{2\sigma^2}} \quad (1)$$

where x is the independent variable for which the function was evaluated, μ is the mean of the distribution, $\sigma$ is the standard deviation.

To generate random values for each independent variable, f (x, μ, $\sigma$) was reformulated to obtain the inverse of the normal distribution function (g (f (x, μ, σ), μ, σ)) as presented in Eq. (2):

$$g(f(x,\mu,\sigma),\mu,\sigma)=\sqrt{2}\,\sigma\left(\mathrm{Ln}\left(\sqrt{2\pi}\,.\,\sigma\,.\,f(x,\mu,\sigma)\right)^2+\mu\right. \quad (2)$$

Fourier's law (Eq. (3)) was used to obtain the relationship between independent and dependent variables:

$$q=\lambda\frac{\Delta T}{L} \quad (3)$$

where q is the heat flux in W/m$^2$, λ is the thermal conductivity value, L is the thickness in m, and ΔT is the difference between the top and bottom surfaces of the specimen in K. ΔT was supposed to be equal to 283.15 K as suggested by other literature [30,40–42] so that the exterior temperature was more than the interior one.

To generate a linear relationship between the water content and thermal conductivity (λ), Eq. (4) is proposed [43–45].

$$\lambda=\lambda_0\left(\left(1+\frac{W}{\rho}\right)\right. \quad (4)$$

where $\lambda_0$ is thermal conductivity value in dry condition (W/m$^2$), W is water content in kg/m$^3$, and ρ is density kg/m$^3$.

Eq. (4) was used to rearrange Eq. (3) as presented in Eq. (5):

$$q=\lambda_0\left(\left(1+\frac{W}{\rho}\right)\frac{\Delta T}{L}\right. \quad (5)$$

Therefore, Eq. (5) was used during the sensitivity analysis process to introduce the relationship between dependent and independent variables.

The coefficient of variation (COV) of independent and dependent variables was calculated using Eq. (6):

$$COV=\frac{\sigma}{\mu} \quad (6)$$

To assess the sensitivity of the dependent variable (q) to the independent variables ($\lambda_0$, W, ρ, and L), it was required to obtain the ratio of COV of q to COV of each independent variable. Increasing this ratio by more than one demonstrates that independent scattering variables lead to the dispersion of q more. While decreasing the ratio above to less than one shows that q is less dispersed and affected once independent variables are scattered.

It is noteworthy that it was essential to control whether the q values based on the specified values in Table 3 were valid or not. Regarding this, after obtaining 5000 random values for each independent variable using Eq. (2), it was controlled whether the calculated q was in its expected range (maximum and minimum values) or not. Less than 1% of q values were out of the expected range. Therefore, q values, obtained based on the specified values for independent variables in Table 3, were valid with more than 99% confidence.

## 3. Results

### 3.1. Validation of green roof models

For green roofs with the drainage layer of IMSWA and LECA, the modeling and experimental results were compared in Fig. 3(a) and 3(b).

As expected, the temperature distribution on green roof models' top and bottom followed the same trend as in roofing systems. For the green roof specimen with the drainage layer of IMSWA, between the substrate

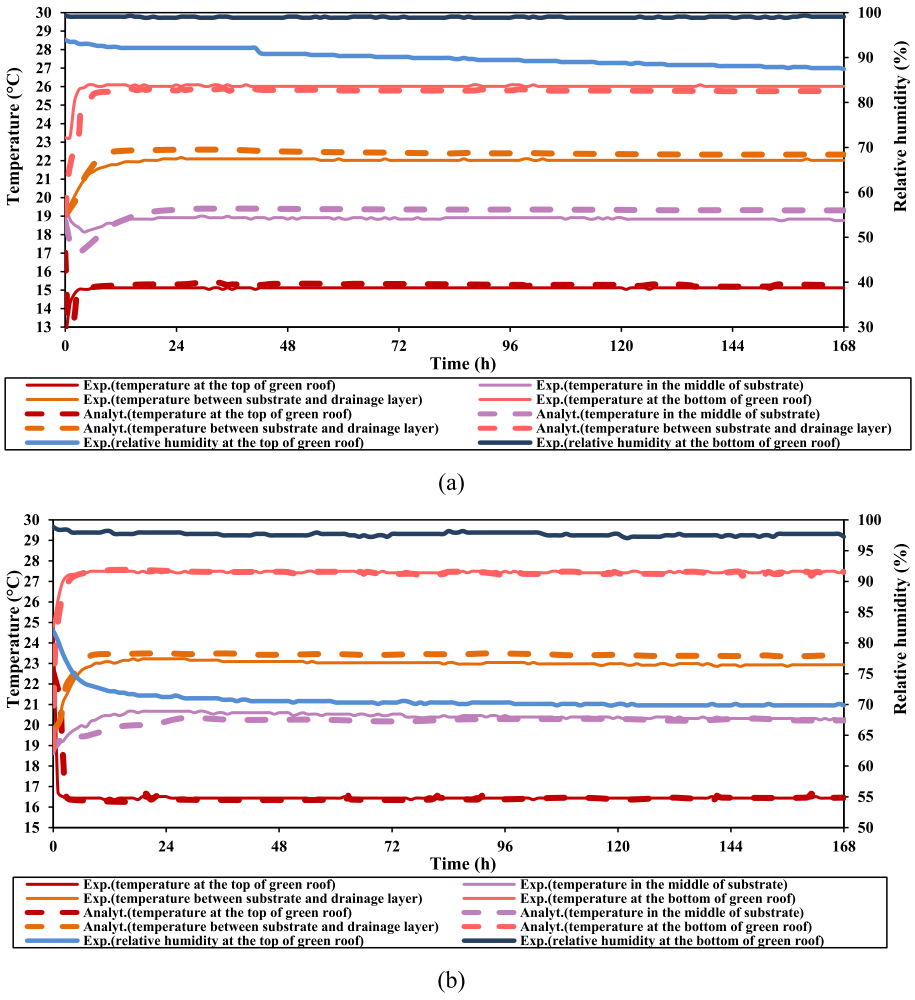


**Fig. 3.** Results from experiments and models for green roofs with the drainage layer of IMSWA (a); and LECA (b). (For interpretation of the references to color in this figure legend, the reader is referred to the Web version of this article.)

and drainage layers and in the middle of the substrate layer, respectively, average temperatures of 22.02 °C and 18.87 °C were reached during the convergence period. For the green roof model, the respective values were 22.39 °C and 19.34 °C. For the green roof specimen with the drainage layer of LECA, during the convergence phase, average temperatures of 22.99 °C and 20.39 °C were attained, respectively, between the substrate and drainage layers and in the middle of the substrate layer. The corresponding temperatures for the green roof model were 23.41 °C and 20.25 °C. The general trend of the temperature distribution through the depth of the green roof models can be said to be almost equivalent to what was seen for the green roof specimens. In addition, comparing the average temperature through the depth of green roof models and specimens showed no greater than a 2.5% difference.

### 3.2. *Effect of weather conditions on green roof models*

The effect of different weather scenarios on temperature and RH variations within the depth of green roof layers was assessed in this study. Also, the results of the water content of drainage and substrate layers under different weather conditions were presented. The outputs regarding heat flux transfer within different green roof models have been compared afterward.

#### 3.2.1. *Temperature and RH variations*

Fig. 4 depicts the temperature and RH variations between the substrate and drainage layers during the 21st century. The temperature and RH fluctuations for green roofs with the SP and green roofs with the SC were nearly identical in each scenario. In scenario 1, the temperature and RH were in the 10.2–27.8 °C and 50–96.8% ranges, respectively. The respective ranges for scenario 2 were 10.8–27.7 °C and 50–98%. These ranges for scenario 3 were 11–27.8 °C and 50–94%. Therefore, all scenarios had nearly the same maximum and minimum temperature and RH between the substrate and drainage layers.

According to Fig. 4(a), in scenario 1, the highest and lowest temperatures between substrate and drainage layers were obtained in August (summer) and March (beginning of spring), respectively. In scenarios 2 and 3 (Fig. 4(b) and 4(c)), the maximum temperatures were in the summer season (from June until August) and at the beginning of autumn (September), while the lowest temperatures were attained in December (beginning of winter). Concerning the RH, the reverse results were observed for all scenarios.

Interior temperature and RH variations for all scenarios are shown in Fig. 5. For scenario 1, RH ranged from 48.2 to 73.1%, and temperature ranged from 17.9 to 25.6 °C, respectively. For scenario 2, the corresponding ranges were 49.9–73% and 18–25.6 °C. These ranges for scenario 3 were 47.5–74% and 18.1–25.8 °C. As recommended by Gilmore [46], the ideal internal RH range for comfort is between 30% and 70%. The results of all scenarios were nearly within the comfort range of RH given by Gilmore [46]. To preserve the health of general populations during cold seasons, a safe and well-balanced indoor temperature is at least 18 °C according to the World Health Organization's 2018 recommendations [47]. Also, healthy sedentary individuals living in an environment with an air temperature between 18 °C and 24 °C do not appear to be at risk for health problems [47]. According to the results, the

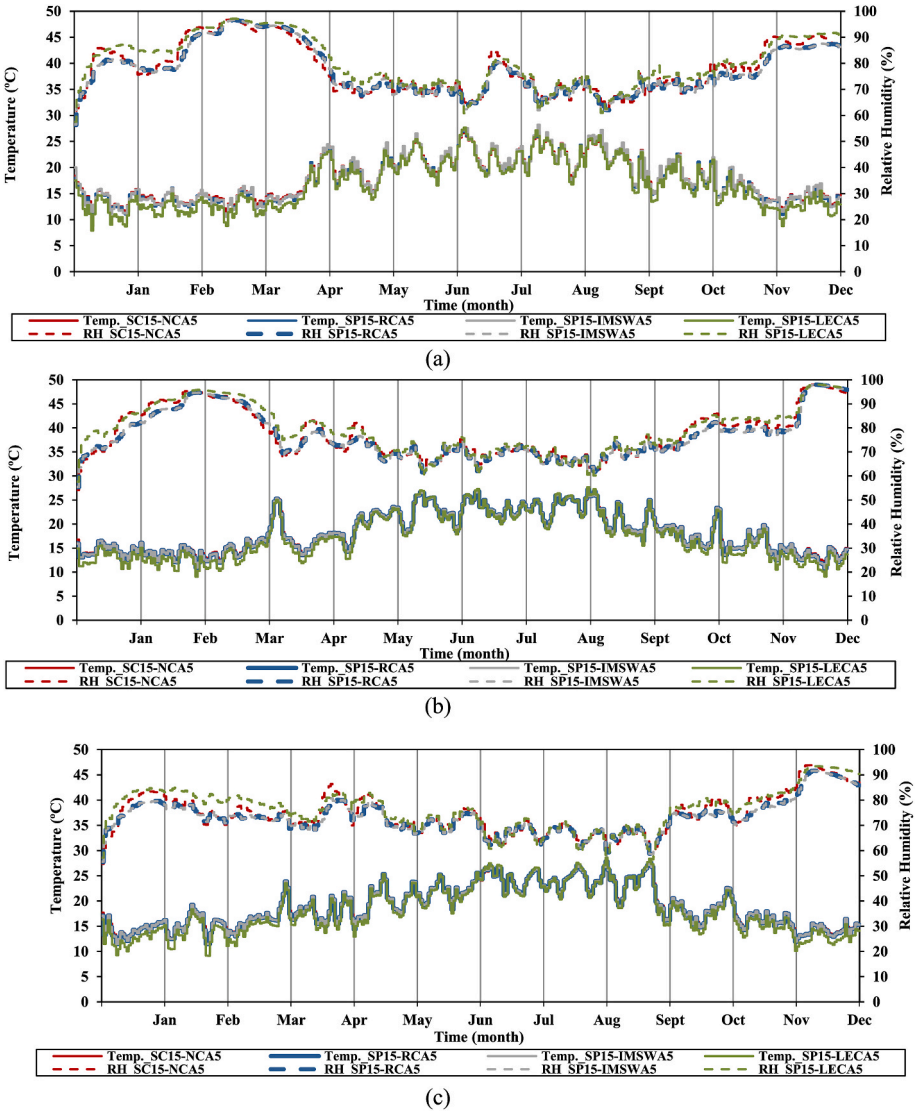


**Fig. 4.** Temperature and RH variations between substrate and drainage layers at the beginning (a); middle (b); end of the 21st century (c).

maximum and minimum range of interior temperatures for all scenarios were obtained near the comfort range given by World Health Organization [47].

In each scenario, nearly the same trends of interior temperature and RH were observed for green roofs with different types of materials. Also, the highest and lowest temperature and RH in the interior surface (Fig. 4 (b)) occurred nearly during the same periods as observed between substrate and drainage layers (Fig. 4(a)). However, the fluctuation of temperature and RH was less in the interior surface than in between substrate and drainage layers. Similar results were found by Parizotto and Lamberts [48] in which the diurnal temperature variation at the lower layers of the green roof systems decreased.

### 3.2.2. *Water content*

The water content values of green roof layers for each month were averagely presented in Fig. 6.

As shown in Fig. 6(a), the water content of SC and SP was averagely obtained at 17.05 and 15.53 kg/m$^3$, respectively, for scenario 1. The respective values for scenario 2 were 18.09 and 16.19 kg/m$^3$. The results for scenario 3 were 11.79 and 9.64 kg/m$^3$. Based on the above, the water content of SC was 13.5% more than that of SP. According to Fig. 6(b), the average water content values of NCA, RCA, IMSWA, and LECA for scenario 1 were 0.8, 2.4, 2, and 2.4 kg/m$^3$, respectively. The corresponding values for scenario 2 were 0.9, 2.5, 2.1, and 2.5 kg/m$^3$. These values for scenario 3 were 0.7, 1.9, 1.6, and 1.9 kg/m$^3$. Therefore, the water content of RCA, IMSWA, and LECA was obtained about 2.5 times more than that of NCA. Similar results were also attained by Kazemi et al. [5] regarding the water retention capacity of the aforementioned coarse granular aggregates.

The water contents of the substrate layer for scenarios 1, 2, and 3 were averagely obtained at about 16.3, 17, and 9.8 kg/m$^3$, respectively. The respective values for drainage materials were 1.9, 2, and 1.5 kg/m$^3$. Therefore, the water content of substrate layers was about nine times more than that of drainage layers for scenarios 1 and 2. The corresponding difference for scenario 3 was 6.5 times.

According to Fig. 6(a), from January to February (winter), the water content of substrate materials increased for scenarios 1 and 2, while the reverse occurred for scenario 3. In March (beginning of spring), a decrease was observed for scenarios 2 and 3, while scenario 1 achieved the highest water content of substrate materials compared to other months. All scenarios experienced a decrease in the water content of substrate materials from March until May (spring). The lowest water content of substrate materials for all scenarios was in the summer season (from June until August) and at the beginning of autumn (September). Then, there was an incremental trend until the end of autumn (from September until November). This trend continued until December (the

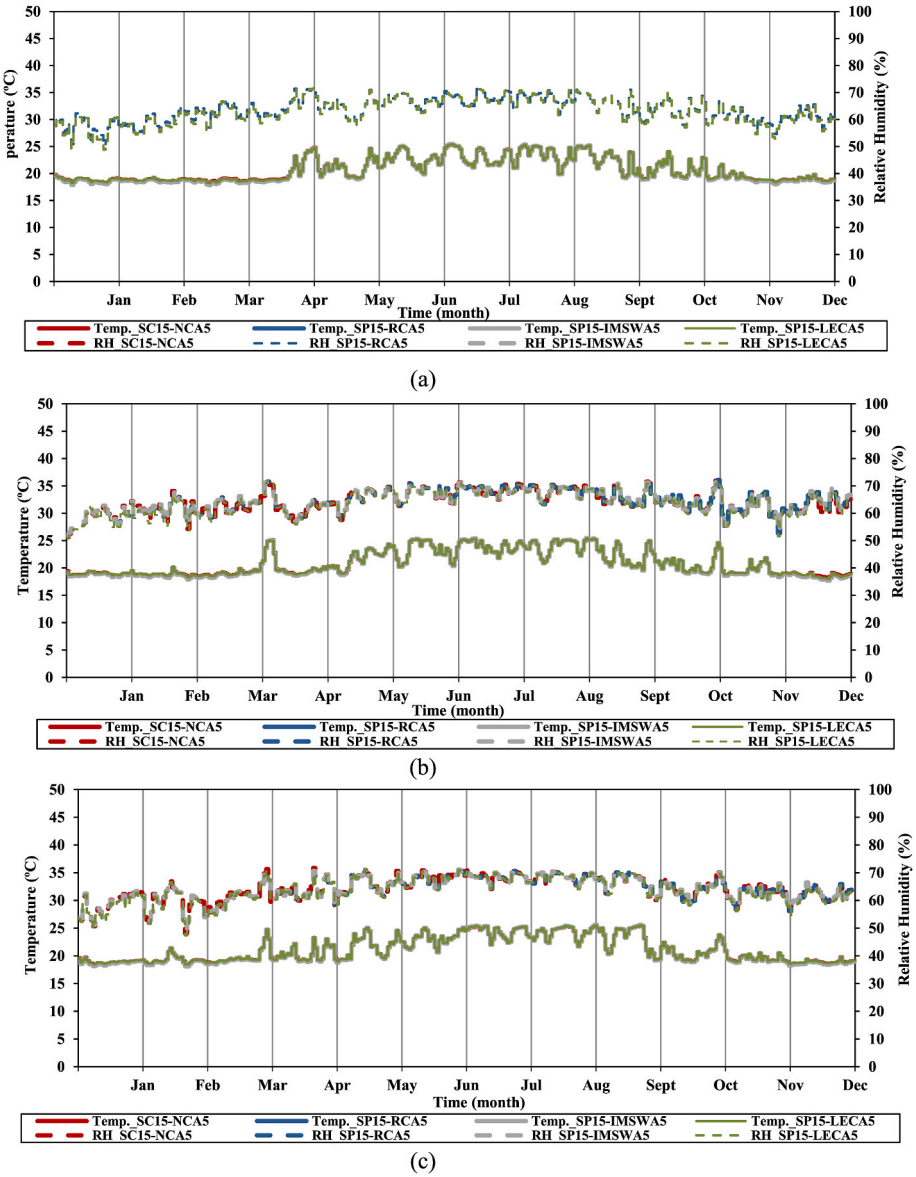


**Fig. 5.** Temperature and RH variations at the bottom of green roof models at the beginning (a); middle (b); end of 21st century (c). (For interpretation of the references to color in this figure legend, the reader is referred to the Web version of this article.)

beginning of winter), when scenarios 2 and 3 had the highest water content of substrate materials compared to other months.

As shown in Fig. 6(b), for all scenarios, the lowest water content of drainage materials was from June until September, similar to what was revealed for substrate materials (Fig. 6(a)). For scenario 1, the highest water content of drainage materials was in March and then April (spring). An increase in the water content of drainage materials for scenario 2 was attained in February and March. Its highest water content was in December, as also observed for scenario 3.

### 3.2.3. Heat flux

The average values of heat flux in each month within the depth of green roof models are presented in Fig. 7.

In the exterior surface (Fig. 7(a)), comparing different scenarios showed that there was a decrease in the heat flux value of scenarios 1 and 2 from January to February (winter), while the reverse was observed for scenario 3. In the spring season, the heat flux increment was experienced from March to May for scenarios 2 and 3, while this increment was observed for scenario 1 until April, and then, there was a decrease in May. In the summer season, there was a fluctuation in heat flux values for scenario 1 from June to August. In the autumn season, scenarios 2 and 3 experienced a reduction in heat flux value from September to November. This trend was followed in December (winter). Generally, the highest and lowest exterior heat flux values of scenario 1 were averagely attained in September and December, respectively (72.5 W/m$^2$ and 18.5 W/m$^2$). For scenario 2, August and December had the highest and lowest exterior heat flux (78.5 W/m$^2$ and 7.5 W/m$^2$), similar to what was observed for scenario 3 (78.5 W/m$^2$ and 13.5 W/m$^2$).

The heat flux values in the interior surface of green roof models are presented in Fig. 7(b). The heat flux values for scenario 1 were averagely obtained at 6.1, 6.6, 6.6, and 5.5 W/m$^2$ for SC15-NCA5, SP15-RCA5, SP15-IMSWA5, and SP15-LECA5, respectively. The respective values for scenario 2 were 5.6, 6.1, 6.1, and 5.1 W/m$^2$. The results of scenario 3 were 4.85, 5.1, 5.1, and 4.2 W/m$^2$. Based on the aforementioned results, the green roof models with the drainage layer of RCA and IMSWA had the same thermal performance in the 21st century. Their heat flux values were 8.2%, 8.9%, and 5.2% more than those of the control green roof model with the drainage layer of NCA in scenarios 1, 2, and 3, respectively. The same trend was observed by Kazemi et al. [5] when they compared the Rc-value of the green roof specimens, including the

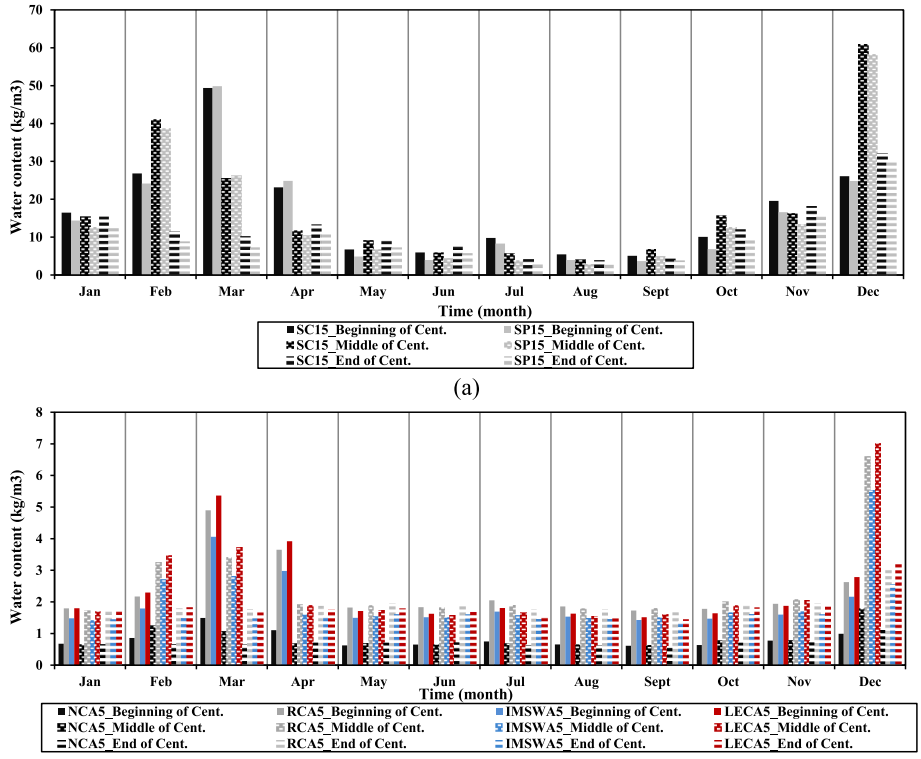


**Fig. 6.** Water content of substrate layers (a); and drainage layers (b).

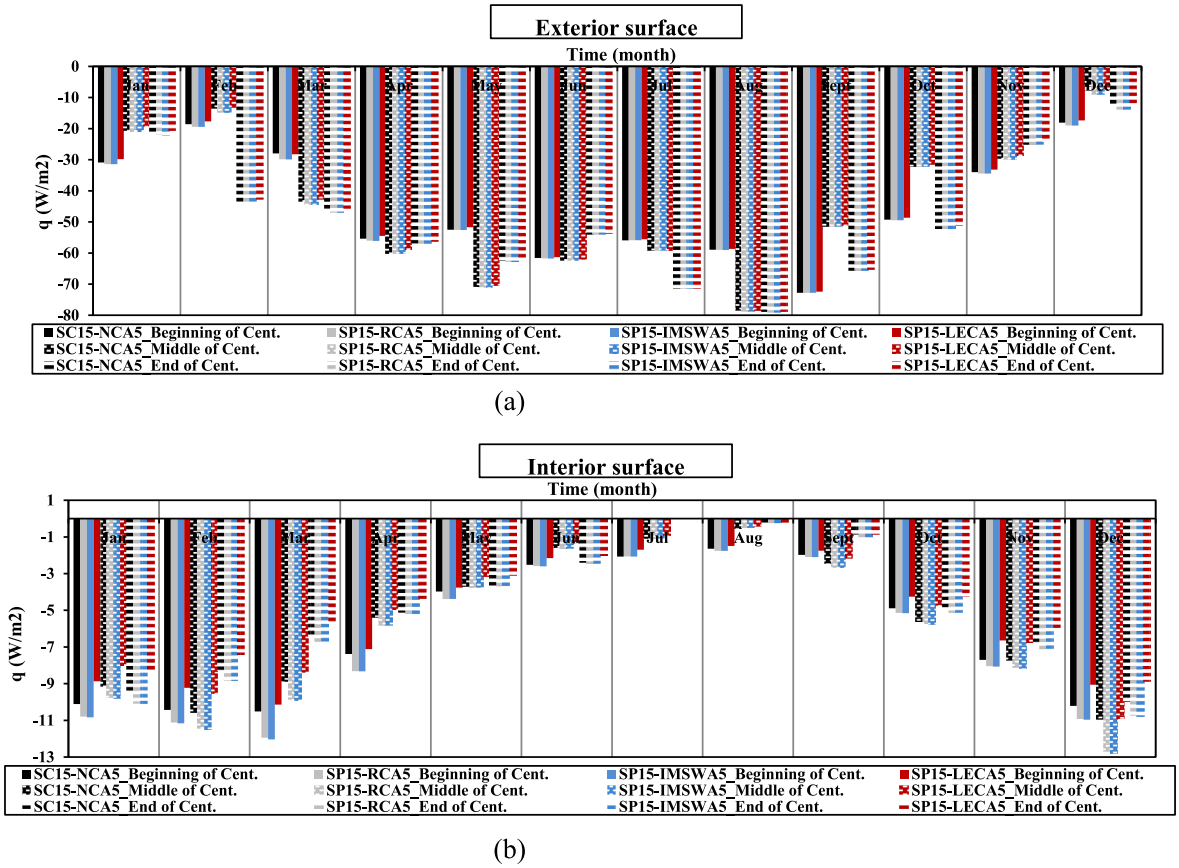


**Fig. 7.** Heat flux on the top of green roof (a); at the bottom of green roof (b). (For interpretation of the references to color in this figure legend, the reader is referred to the Web version of this article.)

drainage layer of RCA and IMSWA, with the control green roof specimen in a wet state.

Therefore, this difference for scenario 1 (8.2%) was nearly the same as scenario 2 (8.9%), demonstrating that the control model with substrate layer of SC and NCA drainage layer moderately had better thermal resistance than green roof models with substrate layer of SP and the drainage layer of RCA and IMSWA. However, decreasing this difference to 5.2% for scenario 3 indicated the better thermal performance of the latter at the end of the 21st century than in other periods. The heat flux values of the green roof model with the drainage layer of LECA were 9.8%, 8.9%, and 13.4% less than those of the control green roof model in scenarios 1, 2, and 3, respectively. The same trend was observed by Kazemi et al. [5]. Hence, the former outperformed the latter in providing thermal resistance for rooftops. Their heat flux differences in scenarios 1 and 2 were nearly the same (9.8% and 8.9%), and increasing this difference in scenario 3 (13.4%) showed better thermal performance of the green roof model with substrate layer of SP and LECA drainage layer at the end of 21st century, similar to what was obtained for green roof models with substrate layer of SP and the drainage layer of RCA and IMSWA.

As shown in Fig. 7(b), the highest and lowest interior heat flux values of scenario 1 were averagely attained in March and August, respectively (11.2 W/m$^2$ and 2 W/m$^2$). Scenario 2 had the highest and lowest interior heat fluxes in December and August (11.9 W/m$^2$ and 0.5 W/m$^2$). In scenario 3, the highest and lowest interior heat fluxes were obtained in December and July (10.1 W/m$^2$ and 0.1 W/m$^2$).

Generally, it can be stated that the interior surface had an incremental heat flux trend during the winter season (December, January, and February) and the beginning of spring (March), while the reverse was observed in the exterior surface. Also, a decreasing heat flux tendency for the interior surface was obtained during the summer (June, July, and August) and at the beginning of autumn (September), contrary to the exterior surface.

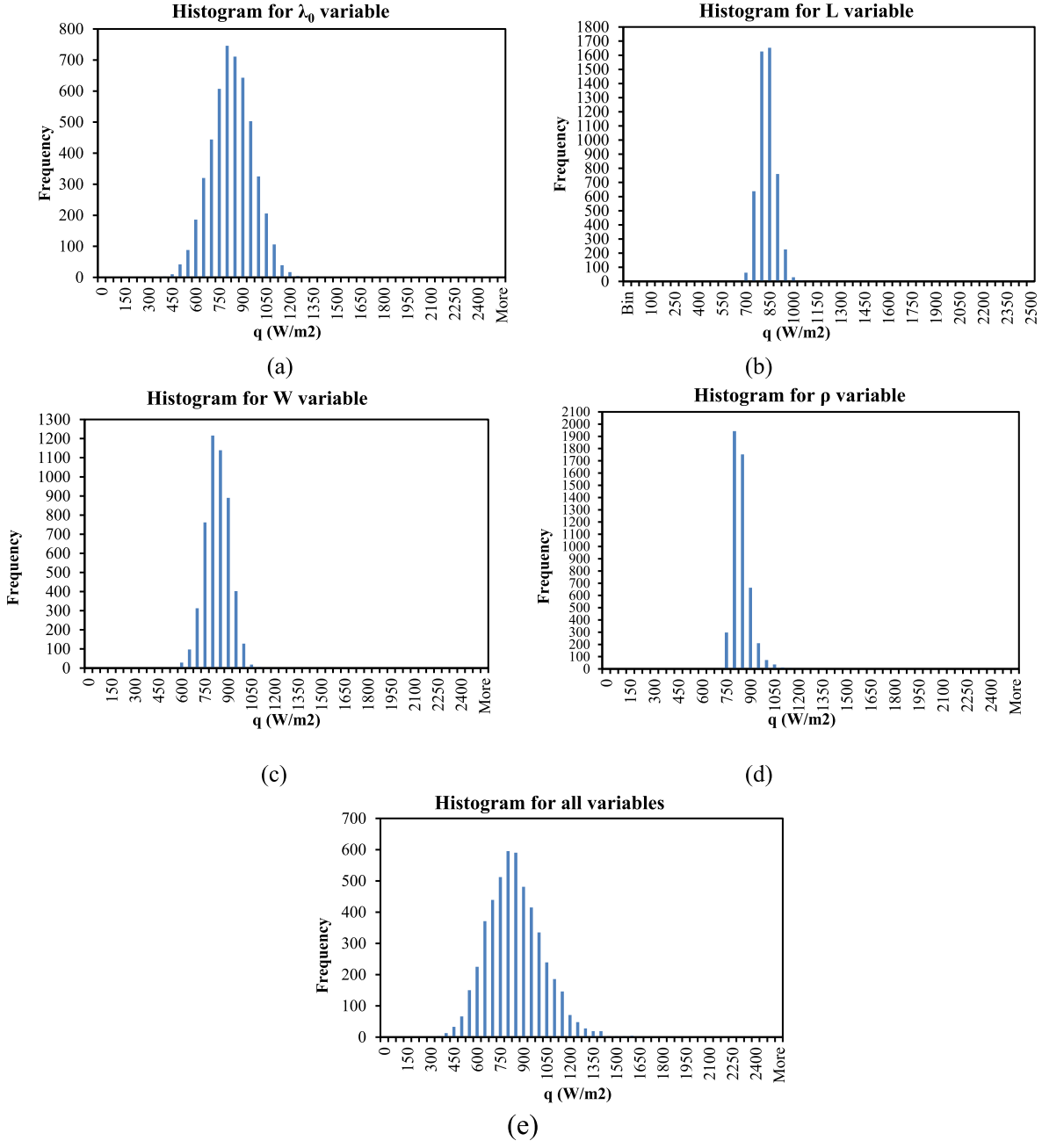


**Fig. 8.** Heat flux histogram of drainage layer for $\lambda_0$ (a); L (b); W (c); ρ (d); and all variables (e).

### 3.3. Sensitivity analysis

Since the maximum and minimum values of independent variables for materials of drainage and substrate layers were different, it was required to perform a separate sensitivity analysis for green roof layers as presented below:

#### 3.3.1. Drainage layer

Fig. 8(a) to 8(d) show the heat flux histograms of the drainage layer for a single independent variable changed while keeping constant other independent variables. The heat flux histogram regarding the entire parameter change is shown in Fig. 8(e). The dispersion of heat flux (q) values had a symmetrical shape in all histograms, demonstrating that all data were well-distributed. Also, only 1% of q values exceeded the expected range. Therefore, there was greater than 99% confidence in the validity of the q values that were calculated using the values for the independent variables in Table 3.

To evaluate the sensitivity of the dependent variable (q) to the independent variables ($\lambda_0$, W, ρ, and L), their COV values for the drainage layer were calculated in the first step. Then, the ratios of COV of q to COV of each independent variable were obtained for both local and global methods, as presented in Table 4. According to the results of the local method, the ratio above for $\lambda_0$ and L was about 1, showing that q was dispersed as much as they were scattered. However, the respective ratio for W and ρ was 0.29, indicating that q was less affected by their dispersion.

As per the results of the global method, the ratios of COV of q to COV of $\lambda_0$, L, W, and ρ were 1.08, 2.69, 0.53, and 0.95. Therefore, the dispersion of q was more and less affected by $\lambda_0$ and W, respectively, similar to the results of the local method. However, due to the hidden interaction among independent variables, q was dispersed as much as ρ scattered in the global method, while the reverse was observed in the local method. Also, the scatter of L dispersed q more, and its effect in the global method was more than that in the local method.

#### 3.3.2. Substrate layer

The heat flux histograms of the substrate layer were obtained using local and global methods, as presented in Fig. 9. Their shapes were symmetrical, similar to what was observed for the drainage layer's histogram. The confidence of q values was high as well (99%).

Table 5 shows COV values of dependent and independent variables for the substrate layer. The ratios of COV of q to COV of $\lambda_0$, W, ρ, and L were 1, 0.95, 0.48, and 0.48. Therefore, the scatter of $\lambda_0$ and L could be equally effective in the dispersion of q, while the influence of ρ, and L was not significant, similar to what was observed for the drainage layer.

In the global method, the ratios of COV of q to COV of $\lambda_0$, L, W, and ρ were 1.27, 2.53, 0.63, and 2.31. Therefore, the dispersion of q for the substrate layer was observed once L was scattered, as also occurred for the drainage layer. Also, the $\lambda_0$ was more effective in the global method than the local method. The W was not effectual in the global method as the local one. However, the hidden interaction among independent variables in the global method remarkably increased the influence of ρ on q scatter, contrary to the local one.

## 4. Discussion

### 4.1. Main findings

The temperature and RH fluctuations between the substrate and drainage layers (Fig. 4) decreased compared to those in the exterior surface (Appendix 1). This could be due to the substrate's significant thermal mass generation near the top of the drainage layer, similar to what Lundholm et al. [49] observed. The RH values were obtained less than 100% in some cases between the substrate and drainage layers owing to air-voids among coarse drainage aggregates. Also, the temperature and RH in the interior surface of green roof models (Fig. 5) were less fluctuated than those between substrate and drainage layers (Fig. 4), so that the former's ranges were attained within the comfort ranges given by World Health Organization [47] and Gilmore [46]. It may be because coarse granular drainage materials had more pores, which created air voids in the drainage layer and increased its heat resistance against fluctuating exterior temperatures. This somewhat prevented the interior temperature from escaping through the green roof's exterior surfaces [8]. Also, the drainage materials offered thermal resistance, preventing the exterior temperature from easily transferring to the interior surface. According to the modeling outputs, most of the time, as the temperature rose, the RH changed quickly. Similar to what Li and Zhu [50] reported, this process could be linked to the evaporation of water content in the substrate layer, which directly impacted heat transfer in the interior surface of green roof systems. As a result of the water in the substrate layer evaporating at high temperatures, the depth of the green roof system was somewhat protected from the transfer of outside temperature and solar radiation.

Due to the green roof layers' high water retention capacity, the interior RH decreased compared to the exterior one. SC's water content was an average of 13.5% higher than SP's (Fig. 6(a)), owing to a large amount of organic matter in the former, leading to slightly more water absorption of the substrate layer. Because of the higher porosity of artificial and recycled drainage aggregates (RCA, IMSWA, and LECA), their water content was about 2.5 times more than that of NCA (Fig. 6 (b)). The presence of fine particles in substrate materials caused their water content to be obtained 9 times more than drainage materials in scenarios 1 and 2. The respective difference in scenario 3 was 6.5 times. The lower difference in scenario 3 was due to less rainfall at the end of the 21st century (Appendix 1).

In comparison to green roof models with a substrate layer of SP and the drainage layer of RCA and IMSWA, the control green roof model with a substrate layer of SC and drainage layer of NCA marginally had greater thermal resistance for all scenarios (Fig. 7). The drainage layer of RCA, IMSWA, and NCA nearly had the same thermal resistance [5]. Therefore, the aforementioned difference could be that the soil's fine particles in SC moderately outperformed coarse recycled materials in SP to prevent heat flux transfer within green roof systems. However, compared to the green roof model with a substrate layer of SP and the drainage layer of LECA, the control green roof model's thermal resistance was lower. Due to the high porosity and low density of LECA as drainage material, its thermal resistance was better than that of NCA [5], similar to what other researchers obtained for other drainage

**Table 4**
COV values of dependent and independent variables for the drainage layer.

| Sensitivity analysis method | Independent variables | COV of independent variables | COV of q | COV of dependent variable (q) / COV of independent variables |
|---|---|---|---|---|
| Local | $\lambda_0$ | 0.167 | 0.167 | 1 |
| | L | 0.067 | 0.067 | 0.97 |
| | W | 0.34 | 0.1 | 0.29 |
| | $\rho$ | 0.19 | 0.055 | 0.29 |
| Global | $\lambda_0$ | 0.167 | 0.18 | 1.08 |
| | L | 0.067 | | 2.69 |
| | W | 0.34 | | 0.53 |
| | $\rho$ | 0.19 | | 0.95 |

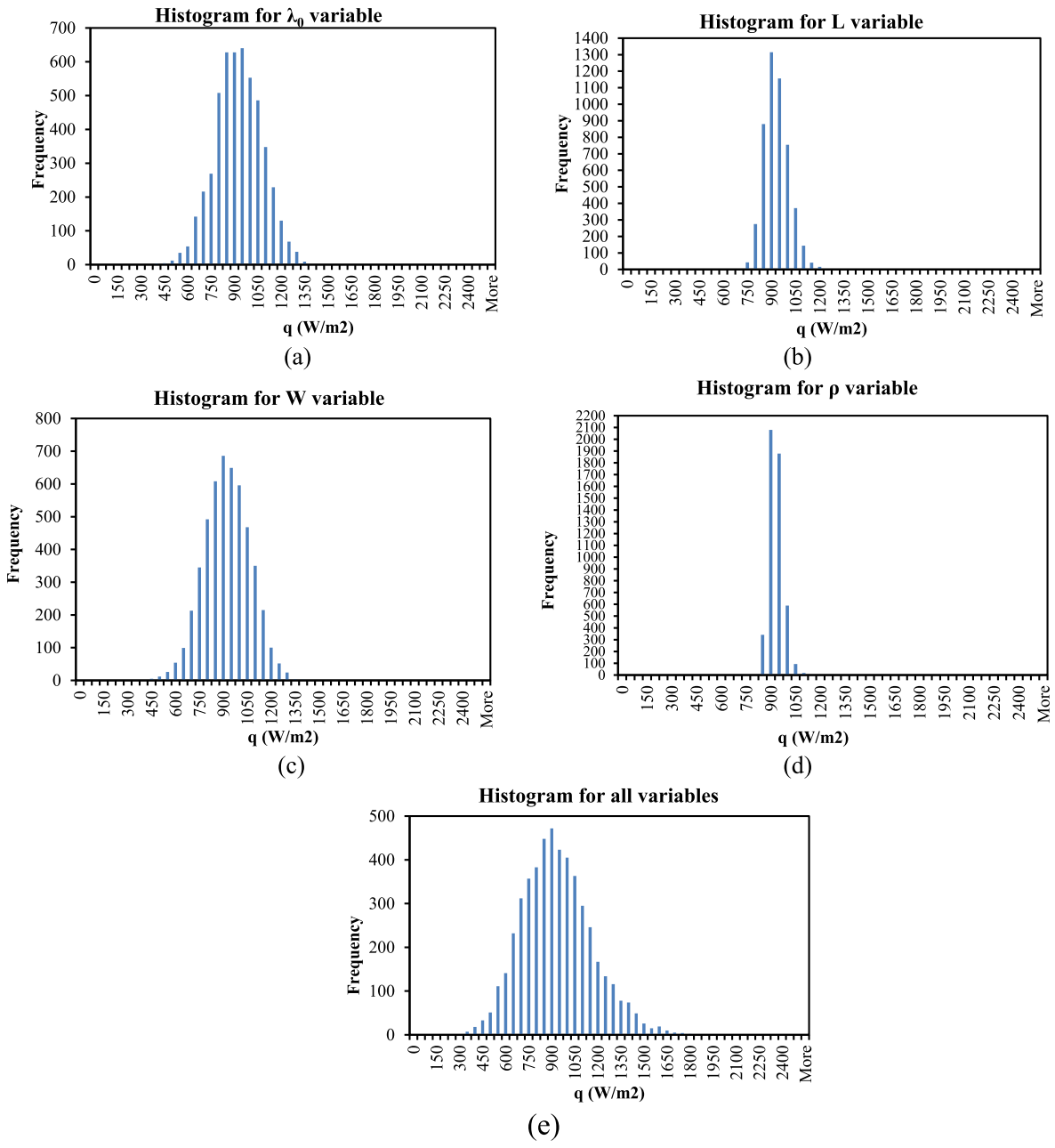


**Fig. 9.** Heat flux histogram of substrate layer for $\lambda_0$ (a); L (b); W (c); ρ (d); and all variables (e).

**Table 5**
COV values of dependent and independent variables for substrate layer.

| Sensitivity analysis method | Independent variables | COV of Independent variables | COV of q | COV of dependent variable (q) / COV of independent variables |
|---|---|---|---|---|
| Local | $\lambda_0$ | 0.165 | 0.165 | 1 |
| | L | 0.083 | 0.079 | 0.952 |
| | W | 0.333 | 0.161 | 0.48 |
| | $\rho$ | 0.091 | 0.044 | 0.48 |
| Global | $\lambda_0$ | 0.165 | 0.21 | 1.27 |
| | L | 0.083 | | 2.53 |
| | W | 0.333 | | 0.63 |
| | $\rho$ | 0.091 | | 2.31 |

aggregates [37,51]. Therefore, in comparison to the substrate layer of SC, the drainage layer of LECA contributed more to providing thermal resistance for green roof systems in the 21st century. Note that the difference between the heat flux of the control green roof model and green roof models with the drainage layer of RCA and IMSWA decreased for scenario 3 compared to scenarios 1 and 2, while this difference between the former and green roof models with the drainage layer of LECA increased. The reason is that the rainfall and, subsequently, water content of green roof layers for scenario 3 (0.015 Ltr/$m^2$) were averagely lower than those for scenarios 1 and 2 (0.022 Ltr/$m^2$). Similar to what

other researchers [26,52–55] reported, decreasing the amount of water content led to increasing air-voids and diffusion properties of artificial and recycled coarse aggregates with high porosity. That's why the substrate layer enhanced the thermal performance of buildings when combined with a drainage layer with a large pore volume, as revealed by Scharf and Zluwa [16]. Therefore, the drainage layer decreased temperature fluctuation and ultimately improved the green roof models' thermal resistance with less rainfall for scenario 3. As a result, since the thermal performance of green roofs with artificial and recycled materials was improved until end of 21st century against the temperate climate, they are recommended to be used for rooftops to apply lower weight to buildings owing to their lower density and higher porosity.

The value of heat flux on the interior surface (Fig. 7(b)) was lower than that on the exterior surface (Fig. 7(a)). This procedure showed that the drainage and substrate layers prevented temperature changes from transferring through the green roof systems, which decreased the diurnal temperature fluctuation at the lower layers of the green roof model [48], leading to decreasing the interior heat flux compared to the exterior one.

In contrast to the exterior surface (Fig. 7(a)), the summer months (June, July, and August) and the beginning of fall (September) had a decreasing heat flow tendency in the interior surface (Fig. 7(b)). Increased temperature caused the water content in the substrate layer to evaporate once there was humidity in the various layers of the green roof during the summer. This evaporated water helped to absorb some of the solar light and temperature outdoors. Considering this, a thermal resistance layer was created in the green roof system due to the moisture in the drainage and substrate layers absorbing the outside temperature to attain a stable temperature [9]. Therefore, increasing solar radiation and air temperature and decreasing RH during the summer led to enhancing green roofs' passive cooling ability, resulting in less heat gain and heat flux [56]. That's why the green roof decreased the cooling energy demand in places with temperate weather, as reported by Ávila-Hernández et al. [57].

The results of the local method (Tables 4 and 5) showed that the q value was scattered as much as the $\lambda_0$ and L dispersed. According to the results of the global method, the drainage and substrate layers' greatest q dispersion was attained once L was scattered, confirming that the thermal resistance of buildings was improved as the green roof construction became thicker, as revealed by Scharf and Zluwa [16]. The ratios of COV of q to COV of $\rho$ showed that the effect of density on q dispersion for the substrate layer (2.31) was higher than that in the drainage layer (0.95). This difference may be because the ranges of maximum and minimum values of other independent variables ($\lambda_0$, W and L) for the substrate layer were greater than those for the drainage layer. This, in turn, increased the effect of hidden interaction among independent variables on the density parameter ($\rho$) to disperse q values more for the substrate layer.

### 4.2. Limitations

There were some limitations that could have affected the outcomes in this study. The influences of plants and their evapotranspiration phenomenon on the hygrothermal performance of green roof models were not considered. Moreover, the color of the soil that could affect the heat flux and the thermal behavior of the green roof layers was not taken into account in the analyses.

## 5. Conclusions

This study assessed the hygrothermal performance of green roof layers, including different coarse artificial and recycled materials, under three weather data scenarios of the 21st century. Sensitivity analysis on drainage and substrate layers made with artificial and recycled components was carried out as well. Based on the presented results, the following conclusions were extracted:

- In comparison to the exterior surface and the area between the substrate and drainage layers, the interior surface presented less temperature and relative humidity fluctuations. Also, for all scenarios, the interior temperature and relative humidity ranges were near to the comfort ranges, providing a healthy internal environment for buildings' occupants.
- Compared to the proposed substrate with coarse recycled materials, the control substrate without coarse recycled materials presented averagely 13.5% more water content by volume. In addition, RCA, IMSWA, and LECA achieved around 2.5 times more water content than NCA. For scenarios 1 and 2, the substrate layers' water content was roughly nine times larger than the drainage layers. For scenario 3, the difference was 6.5 times larger owing to lower rainfall at the end of the 21st century.
- The lowest water content of green roof materials for all scenarios happened in the summer and at the beginning of autumn. For scenario 1, the highest water content of green roof materials happened in March and April (spring). With scenarios 2 and 3, the highest water content was observed in December (winter).
- The lowest interior heat flow values for scenarios 1 and 2 were observed in August. July experienced the same for scenario 3. March had the highest interior heat flow values for scenario 1. The same was observed in December for scenarios 2 and 3.
- During the summer months and the beginning of autumn, a decrease in the rainfall pattern until the end of the 21st century caused the heat resistance of green roof models with artificial and recycled materials to increase for scenario 3, compared to scenarios 1 and 2.
- Decreasing heat flow tendency in the interior surface during the summer months and the beginning of fall revealed the passive cooling ability of green roof models.
- The sensitivity to a single independent variable revealed that the highest dispersion of q for the green roof layers was attained when $\lambda_0$ and L changed. However, the former was less affected by the W and $\rho$ scatter.
- The entire parameters change showed that the scatter of $\lambda_0$, $\rho$, and L influenced the dispersion of q for the green roof layers. However, the scatter of $\rho$ was more effective in the dispersion of q for the substrate layer than the drainage layer.

Therefore, using artificial and recycled components seems to improve the thermal performances of green roof systems against the temperate climate until the end of the 21st century and has a positive effect on buffering climate change for housing comfort.

## CRediT authorship contribution statement

**Mostafa Kazemi:** Writing – original draft, Visualization, Validation, Software, Methodology, Investigation, Formal analysis, Data curation, Conceptualization. **Ramin Rahif:** Writing – review & editing. **Luc Courard:** Writing – review & editing, Supervision, Funding acquisition. **Shady Attia:** Writing – review & editing, Supervision.

## Declaration of competing interest

The authors declare that they have no known competing financial interests or personal relationships that could have appeared to influence the work reported in this paper.

## Data availability

No data was used for the research described in the article.

## Acknowledgments

This research was funded through the University of Liège and ARC grant for Concerted Research Actions, financed by the French Community of Belgium, Wallonia-Brussels Federation (CityRoof project: Analogous green roofs for urban ecosystem services (2020–2023)).

## Appendix 1

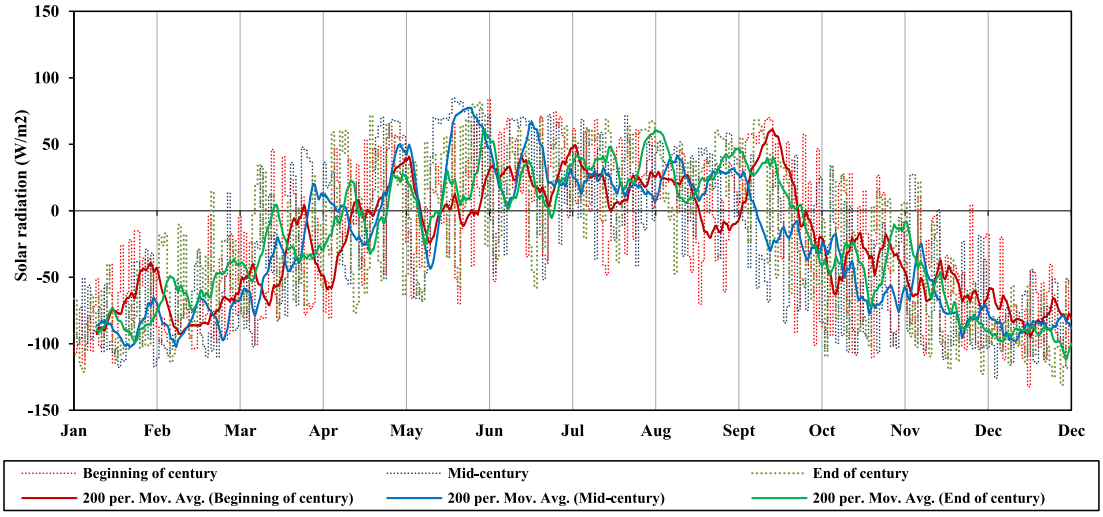


(a)

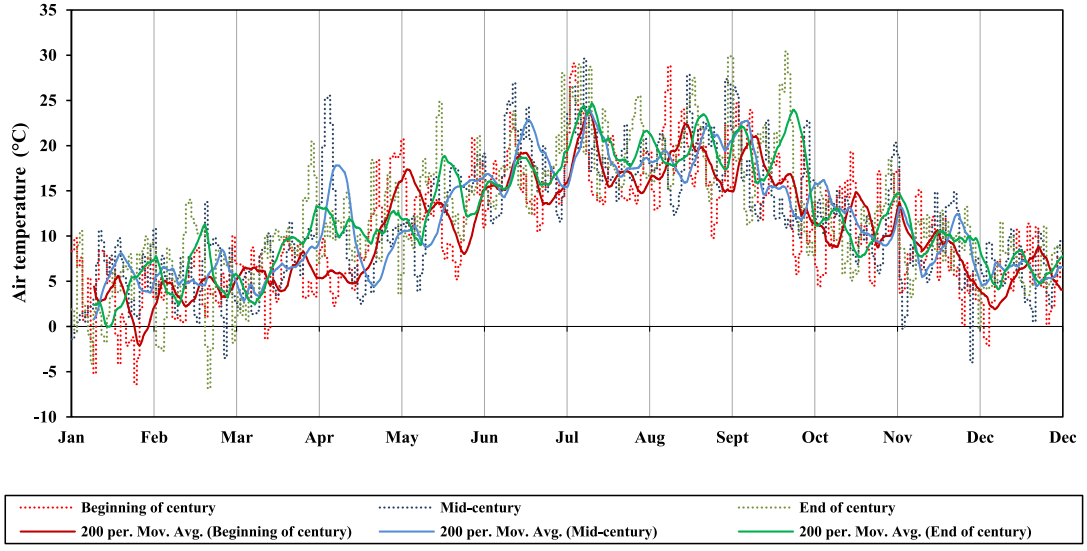


(b)

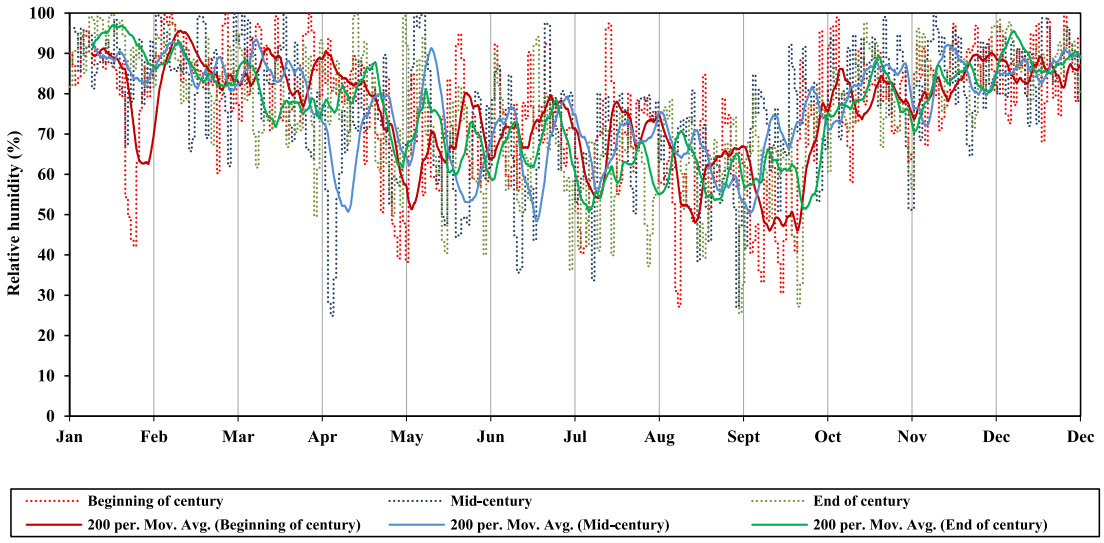


(c)

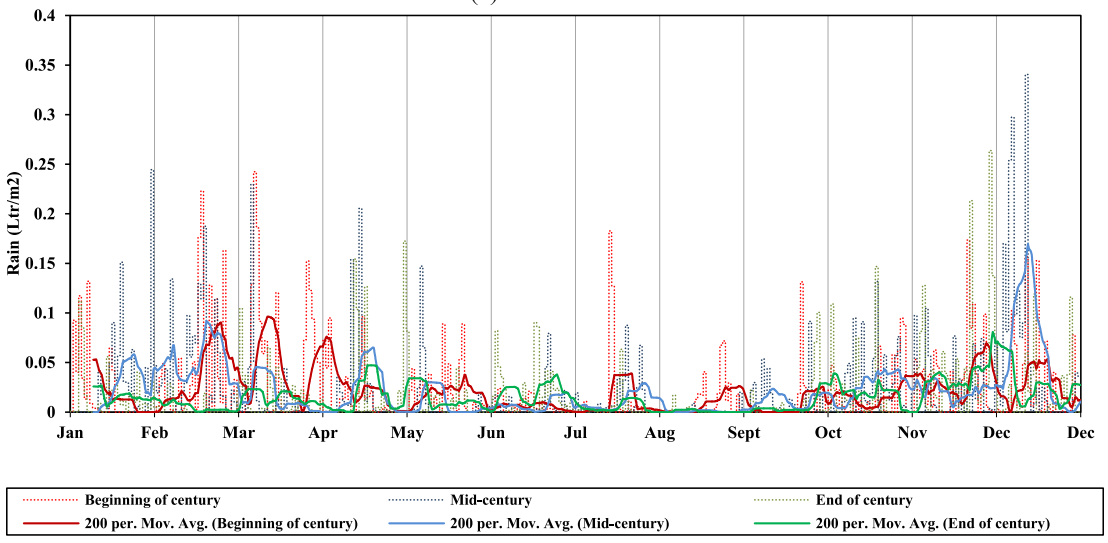


(d)

(*continued*).

## References


[1] M. Zhao, J. Srebric, Assessment of green roof performance for sustainable buildings under winter weather conditions, J. Cent. South Univ. Technol. 19 (2012) 639–644, https://doi.org/10.1007/s11771-012-1050-1.

[2] F. Tariku, S. Hagos, Performance of green roof installed on highly insulated roof deck and the plants' effect: an experimental study, Build. Environ. 221 (2022), 109337, https://doi.org/10.1016/j.buildenv.2022.109337.

[3] G. Peri, G.R. Licciardi, N. Matera, D. Mazzeo, L. Cirrincione, G. Scaccianoce, Disposal of green roofs: a contribution to identifying an "Allowed by legislation" end–of–life scenario and facilitating their environmental analysis, Build. Environ. 226 (2022), 109739, https://doi.org/10.1016/j.buildenv.2022.109739.

[4] L. Cirrincione, A. Marvuglia, G. Scaccianoce, Assessing the effectiveness of green roofs in enhancing the energy and indoor comfort resilience of urban buildings to climate change: Methodology proposal and application, Build. Environ. 205 (2021), 108198, https://doi.org/10.1016/j.buildenv.2021.108198.

[5] M. Kazemi, L. Courard, S. Attia, Water permeability, water retention capacity, and thermal resistance of green roof layers made with recycled and artificial aggregates, Build. Environ. 227 (2023), 109776, https://doi.org/10.1016/j.buildenv.2022.109776.

[6] M. Kazemi, L. Courard, Modelling hygrothermal conditions of unsaturated substrate and drainage layers for the thermal resistance assessment of green roof: effect of coarse recycled materials, Energy Build. 250 (2021), 111315, https://doi.org/10.1016/j.enbuild.2021.111315.

[7] L. Tams, T. Nehls, C.S.C. Calheiros, Rethinking green roofs- natural and recycled materials improve their carbon footprint, Build. Environ. 219 (2022), 109122, https://doi.org/10.1016/j.buildenv.2022.109122.

[8] J. Coma, G. Pérez, C. Solé, A. Castell, L.F. Cabeza, Thermal assessment of extensive green roofs as passive tool for energy savings in buildings, Renew. Energy 85 (2016) 1106–1115, https://doi.org/10.1016/j.renene.2015.07.074.

[9] M. Kazemi, L. Courard, Simulation of humidity and temperature distribution in green roof with pozzolana as drainage layer: influence of outdoor seasonal weather conditions and internal ceiling temperature, Sci. Technol. Built. Environ.t 27 (2021) 509–523, https://doi.org/10.1080/23744731.2021.1873658.

[10] P.M. Klein, R. Coffman, Establishment and performance of an experimental green roof under extreme climatic conditions, Sci. Total Environ. (2015) 82–93, https://doi.org/10.1016/j.scitotenv.2015.01.020, 512–513.

[11] G. Pérez, A. Vila, L. Rincón, C. Solé, L.F. Cabeza, Use of rubber crumbs as drainage layer in green roofs as potential energy improvement material, Appl. Energy 97 (2012) 347–354, https://doi.org/10.1016/j.apenergy.2011.11.051.

[12] K. Zhang, A. Garg, G. Mei, M. Jiang, H. Wang, S. Huang, L. Gan, Thermal performance and energy consumption analysis of eight types of extensive green roofs in subtropical monsoon climate, Build. Environ. 216 (2022), 108982, https://doi.org/10.1016/j.buildenv.2022.108982.

[13] K.L. Getter, D.B. Rowe, J.A. Andresen, I.S. Wichman, Seasonal heat flux properties of an extensive green roof in a Midwestern U.S. climate, Energy Build. 43 (2011) 3548–3557, https://doi.org/10.1016/j.enbuild.2011.09.018.

[14] P. Stella, E. Personne, Effects of conventional, extensive and semi-intensive green roofs on building conductive heat fluxes and surface temperatures in winter in Paris, Build. Environ. 205 (2021), 108202, https://doi.org/10.1016/j.buildenv.2021.108202.

[15] V. Sandoval, C.A. Bonilla, J. Gironás, S. Vera, F. Victorero, W. Bustamante, V. Rojas, E. Leiva, P. Pastén, F. Suárez, Porous media characterization to simulate water and heat transport through green roof substrates, Vadose Zone J. 16 (2017), https://doi.org/10.2136/vzj2016.10.0101 vzj2016.10.0101.

[16] B. Scharf, I. Zluwa, Case study investigation of the building physical properties of seven different green roof systems, Energy Build. 151 (2017) 564–573, https://doi.org/10.1016/j.enbuild.2017.06.050.
[17] Y. Zhang, L. Zhang, L. Ma, Q. Meng, P. Ren, Cooling benefits of an extensive green roof and sensitivity analysis of its parameters in subtropical areas, Energies 12 (2019) 4278, https://doi.org/10.3390/en12224278.
[18] C. Van Mechelen, T. Dutoit, M. Hermy, Adapting green roof irrigation practices for a sustainable future: a review, Sustain. Cities Soc. 19 (2015) 74–90, https://doi.org/10.1016/j.scs.2015.07.007.
[19] A.L.S. Chan, T.T. Chow, Energy and economic performance of green roof system under future climatic conditions in Hong Kong, Energy Build. 64 (2013) 182–198, https://doi.org/10.1016/j.enbuild.2013.05.015.
[20] A. Nagase, Novel application and reused materials for extensive green roof substrates and drainage layers in Japan – plant growth and moisture uptake implementation, Ecol. Eng. 153 (2020), 105898, https://doi.org/10.1016/j.ecoleng.2020.105898.
[21] M. Eksi, O. Sevgi, S. Akburak, H. Yurtseven, İ. Esin, Assessment of recycled or locally available materials as green roof substrates, Ecol. Eng. 156 (2020), 105966, https://doi.org/10.1016/j.ecoleng.2020.105966.
[22] S. Cascone, Green roof design: state of the art on technology and materials, Sustainability 11 (2019) 1–27.
[23] S.B. Mickovski, K. Buss, B.M. McKenzie, B. Sökmener, Laboratory study on the potential use of recycled inert construction waste material in the substrate mix for extensive green roofs, Ecol. Eng. 61 (2013) 706–714, https://doi.org/10.1016/j.ecoleng.2013.02.015.
[24] C.J. Molineux, A.C. Gange, S.P. Connop, D.J. Newport, Using recycled aggregates in green roof substrates for plant diversity, Ecol. Eng. 82 (2015) 596–604, https://doi.org/10.1016/j.ecoleng.2015.05.036.
[25] A.J. Bates, J.P. Sadler, R.B. Greswell, R. Mackay, Effects of recycled aggregate growth substrate on green roof vegetation development: a six year experiment, Landsc. Urban Plann. 135 (2015) 22–31, https://doi.org/10.1016/j.landurbplan.2014.11.010.
[26] L. Rincón, J. Coma, G. Pérez, A. Castell, D. Boer, L.F. Cabeza, Environmental performance of recycled rubber as drainage layer in extensive green roofs. A comparative Life Cycle Assessment, Build. Environ. 74 (2014) 22–30, https://doi.org/10.1016/j.buildenv.2014.01.001.
[27] M. Shafique, A. Azam, M. Rafiq, M. Ateeq, X. Luo, An overview of life cycle assessment of green roofs, J. Clean. Prod. 250 (2020), 119471, https://doi.org/10.1016/j.jclepro.2019.119471.
[28] T.P. Scolaro, E. Ghisi, Life cycle assessment of green roofs: a literature review of layers materials and purposes, Sci. Total Environ. 829 (2022), 154650, https://doi.org/10.1016/j.scitotenv.2022.154650.
[29] M. Kazemi, L. Courard, J. Hubert, Heat transfer measurement within green roof with incinerated municipal solid waste aggregates, Sustainability 13 (2021) 7115, https://doi.org/10.3390/su13137115.
[30] M. Kazemi, L. Courard, J. Hubert, Coarse recycled materials for the drainage and substrate layers of green roof system in dry condition: parametric study and thermal heat transfer, J. Build. Eng. 45 (2022), 103487, https://doi.org/10.1016/j.jobe.2021.103487.
[31] FLL Guidelines, Guidelines for the Planning, Construction and Maintenance of Green Roofing: Green Roofing Guideline, 2008.
[32] S. Doutreloup, X. Fettweis, R. Rahif, E.A. Elnagar, M.S. Pourkiaei, D. Amaripadath, S. Attia, Historical and future weather data for dynamic building simulations in Belgium using the MAR model: typical & extreme meteorological year and heatwaves, Earth Syst. Sci. Data Discuss. (2022) 1–19.
[33] C.S. Barnaby, U.B. Crawley, Weather data for building performance simulation, in: Building Performance Simulation for Design and Operation, Routledge, 2012, pp. 61–79.
[34] S. Wilcox, W. Marion, Users Manual for TMY3 Data Sets, 2008.
[35] EN 15026, Hygrothermal Performance of Building Components and Building Elements. Assessment of Moisture Transfer by Numerical Simulation, 2007.
[36] W.A. Mahar, G. Verbeeck, S. Reiter, S. Attia, Sensitivity analysis of passive design strategies for residential buildings in cold semi-arid climates, Sustainability 12 (2020) 1091, https://doi.org/10.3390/su12031091.
[37] J. Coma, G. Pérez, A. Castell, C. Solé, L.F. Cabeza, Green roofs as passive system for energy savings in buildings during the cooling period: use of rubber crumbs as drainage layer, Energy Efficiency 7 (2014) 841–849, https://doi.org/10.1007/s12053-014-9262-x.
[38] A. Teemusk, Ü. Mander, Greenroof potential to reduce temperature fluctuations of a roof membrane: a case study from Estonia, Build. Environ. 44 (2009) 643–650, https://doi.org/10.1016/j.buildenv.2008.05.011.
[39] H.J. Ladani, J.-R. Park, Y.-S. Jang, H.-S. Shin, Hydrological performance assessment for green roof with various substrate depths and compositions, KSCE J. Civ. Eng. 23 (2019) 1860–1871, https://doi.org/10.1007/s12205-019-0270-4.
[40] G. Desogus, S. Mura, R. Ricciu, Comparing different approaches to in situ measurement of building components thermal resistance, Energy Build. 43 (2011) 2613–2620, https://doi.org/10.1016/j.enbuild.2011.05.025.
[41] ISO 9869-1, Building elements, In-Situ Measurement of Thermal Resistance and Thermal Transmittance-Part 1: Heat Flow Meter Method, 2014.
[42] P. La Roche, U. Berardi, Comfort and energy savings with active green roofs, Energy Build. 82 (2014) 492–504, https://doi.org/10.1016/j.enbuild.2014.07.055.
[43] M. Vertaľ, M. Zozulák, A. Vašková, A. Korjenic, Hygrothermal initial condition for simulation process of green building construction, Energy Build. 167 (2018) 166–176, https://doi.org/10.1016/j.enbuild.2018.02.004.
[44] D. Allinson, M. Hall, Hygrothermal analysis of a stabilised rammed earth test building in the UK, Energy Build. 42 (2010) 845–852, https://doi.org/10.1016/j.enbuild.2009.12.005.
[45] L. Veas, Development and Application of a Methodological Model that Allows Evaluate and Compare the Behaviour of External Walls Exposed to Moisture Phenomenons, 2006. PhD Thesis, UCLouvain.
[46] C.P. Gilmore, More comfort for your heating dollar, Popular Sci. 99 (1972).
[47] WHO, WHO Housing and Health Guidelines, 2018.
[48] S. Parizotto, R. Lamberts, Investigation of green roof thermal performance in temperate climate: a case study of an experimental building in Florianópolis city, Southern Brazil, Energy Build. 43 (2011) 1712–1722, https://doi.org/10.1016/j.enbuild.2011.03.014.
[49] J.T. Lundholm, B.M. Weddle, J.S. MacIvor, Snow depth and vegetation type affect green roof thermal performance in winter, Energy Build. 84 (2014) 299–307, https://doi.org/10.1016/j.enbuild.2014.07.093.
[50] Y. Li, Q. Zhu, Simultaneous heat and moisture transfer with moisture sorption, condensation, and capillary liquid diffusion in porous textiles, Textil. Res. J. (2016) 73. https://journals.sagepub.com/doi/abs/10.1177/004051750307300609. (Accessed 11 January 2023).
[51] G. Pérez, J. Coma, C. Solé, A. Castell, L.F. Cabeza, Green roofs as passive system for energy savings when using rubber crumbs as drainage layer, Energy Proc. 30 (2012) 452–460, https://doi.org/10.1016/j.egypro.2012.11.054.
[52] A. Shadmani, B. Tahmouresi, A. Saradar, E. Mohseni, Durability and microstructure properties of SBR-modified concrete containing recycled asphalt pavement, Construct. Build. Mater. 185 (2018) 380–390, https://doi.org/10.1016/j.conbuildmat.2018.07.080.
[53] M. Koushkbaghi, P. Alipour, B. Tahmouresi, E. Mohseni, A. Saradar, P.K. Sarker, Influence of different monomer ratios and recycled concrete aggregate on mechanical properties and durability of geopolymer concretes, Construct. Build. Mater. 205 (2019) 519–528, https://doi.org/10.1016/j.conbuildmat.2019.01.174.
[54] M. Eskandarinia, M. Esmailzade, A. Hojatkashani, A. Rahmani, S. Jahandari, Optimized alkali-activated slag-based concrete reinforced with recycled tire steel fiber, Materials 15 (2022) 6623, https://doi.org/10.3390/ma15196623.
[55] S. Jahandari, M. Mohammadi, A. Rahmani, M. Abolhasani, H. Miraki, L. Mohammadifar, M. Kazemi, M. Saberian, M. Rashidi, Mechanical properties of recycled aggregate concretes containing silica fume and steel fibres, Materials 14 (2021) 7065, https://doi.org/10.3390/ma14227065.
[56] C.Y. Jim, L.L.H. Peng, Weather effect on thermal and energy performance of an extensive tropical green roof, Urban For. Urban Green. 11 (2012) 73–85, https://doi.org/10.1016/j.ufug.2011.10.001.
[57] A. Ávila-Hernández, E. Simá, J. Xamán, I. Hernández-Pérez, E. Téllez-Velázquez, M.A. Chagolla-Aranda, Test box experiment and simulations of a green-roof: thermal and energy performance of a residential building standard for Mexico, Energy Build. 209 (2020), 109709, https://doi.org/10.1016/j.enbuild.2019.109709.